

Polymorphic Crystallization and Structural Aspects of Agomelatine Metastable Form X Prepared by Combined Antisolvent/Cooling Process

Jan Holaň,^{†,‡} Eliška Skořepová,^{‡,§} Lea Heraud,^{||,⊥} David Baltes,^{||} Jan Rohlíček,[§] Ondřej Dammer,[‡] Luděk Ridvan,[‡] and František Štěpánek*,[†]

[†]Department of Chemical Engineering and [§]Department of Solid State Chemistry, University of Chemistry and Technology Prague, Technická 5, 166 28 Prague 6, Czech Republic

[‡]Zentiva k.s., U Kabelovny 130/22, 102 00 Prague 10, Czech Republic

^{||}Sanofi SA, 45 Chemin de Météline, Sisteron, 04200, France

[⊥]Ecole Nationale Supérieure des Ingénieurs en Arts Chimiques et Technologiques, 4 Allée Émile Monso, 31030 Toulouse, France

ABSTRACT: Polymorphism is of great interest to the pharmaceutical industry because polymorphs have different physicochemical properties such as dissolution rate. In the present work, the influence of process conditions on the polymorphic antisolvent crystallization and transformations during cooling crystallization of agomelatine metastable form X from water/methanol solution has been investigated with a view of designing a robust process that includes not only crystallization but also filtration, filter cake washing, and drying. The competitive stability method was used in order to identify regions of the parametric space (water/methanol ratio, process temperature, and initial concentration) in which the crystallization of form X can be feasible. The formation of agomelatine form X was confirmed by subsequent kinetic experiments. The influence of process parameters such as the intensity of agitation, the antisolvent addition rate, and the precipitation temperature on the yield and particle size of the crystalline product was also investigated. The batch antisolvent crystallization of the metastable form X was monitored using in-line Raman spectroscopy and FBRM probe, and the type of the resulting polymorph has been confirmed by X-ray powder diffraction (XRPD). Finally, the effect of the obtained crystals of metastable form X on downstream operations—namely, filtration and drying—has been studied.

1. INTRODUCTION

Polymorphism is of great interest to the pharmaceutical industry because polymorphs have different physicochemical properties including solubility and dissolution rate, which may affect bioavailability, compaction, flow, and stability.^{1,2} Polymorphism is defined as the ability of a single constituent to exist in more than one crystallographic arrangement. The study of polymorphism with regard to small organic molecules, representing the active pharmaceutical ingredients (APIs), has become an increasingly important research topic in the area of both chemical engineering and industrial pharmacy. It has been reported that approximately 80% of marketed pharmaceuticals exhibit polymorphism.³ The relative stability of the polymorphs is defined by thermodynamics, but the formation of actual polymorphic form depends also on the kinetics of nucleation and subsequent crystal growth, which can be controlled by the crystallization process conditions.⁴

The driving force for crystallization from solution is supersaturation of the mother liquor, which can be achieved by evaporation, cooling, or the addition of an antisolvent.⁵ The principle of antisolvent crystallization is based on reducing the solubility of the dissolved compound by changing the solvent composition. Antisolvent crystallization is a widely used method for crystallizing metastable forms. According to the Ostwald's rule of stages, a metastable polymorph forms first at higher supersaturation, followed by transformation to a more stable polymorph at lower supersaturation.^{1,2} Therefore, the

knowledge of the polymorphic form stability at the desired temperatures in a suspension is crucial for the design a robust crystallization process.

There are two types of polymorphism from the thermodynamic viewpoint: monotropy and enantiotropy.⁶ In the case of a monotropic system, one polymorph is the stable solid modification over the entire temperature range up to the melting point. Therefore, there is no transition point below the melting point, and the ability to crystallize the less stable polymorph strongly depends on the chosen solvent. In the case of an enantiotropic system, a reversible transition point (equilibrium point) exists at some temperature below the melting point of the crystal. In the enantiotropic system, one polymorph is more stable in a temperature range below the equilibrium point and less stable above it.⁷ Robust crystallization of the required polymorph is usually more feasible in this case, as the preferred polymorph can be selected by the choice of temperature.

When the crystal structures of various polymorphs of a given compound are available, a simple rule can be used to determine their relative thermodynamic stability.^{8,9} It was postulated by Kitaigorodskii⁸ that, in systems that lack hydrogen bonds, the more densely the structure is packed, the higher its stability ("density rule"). However, there are also exceptions to this rule,

Received: July 28, 2015

Published: November 30, 2015



perhaps the most well-known one being paracetamol whose most stable polymorph has a significantly lower density than the metastable one.¹⁰ The stability and transition points can be estimated from the melting points and heats of fusion of the individual polymorphic forms according to the following expression,¹¹

$$T_t = \frac{\Delta H_{f,I} - \Delta H_{f,II}}{\Delta H_{f,I}/T_{mp,I} - \Delta H_{f,II}/T_{mp,II}} \quad (1)$$

where T_t (K) is the transition point, $T_{mp,I}$ and $T_{mp,II}$ are the melting points of the two polymorphic forms, and $\Delta H_{f,I}$ and $\Delta H_{f,II}$ are their heats of fusion, respectively. Eq 1 involves an assumption that the heat of fusion is constant with temperature. The polymorph with a higher T_{mp} is most likely to be the more stable form at lower temperatures. If the higher-melting polymorph also has a higher ΔH_f , then that polymorph is almost certainly the most stable form at lower temperatures. However, if the lower-melting polymorph has the higher ΔH_f , then the transition point between the two forms exists at some temperature below the melting point.⁷

While the estimation of relative stability of polymorphs using the above method involves solid phase characterization by differential scanning calorimetry (DSC) to obtain the melting points and enthalpies of fusion, the measurement of polymorph solubility by the so-called competitive stability (ripening) method can be used as an alternative approach.¹² The competitive stability method includes the solubility measurement of a polymorphic mixture. The combination of two or more polymorphic forms is stirred in a suspension until the equilibrium state is reached. The solution and the filtered material are then analyzed and the resulting polymorphic form is the more stable one at given conditions. The competitive stability measured at several temperatures and solvent/antisolvent ratio may provide useful information about conditions suitable for the design of the polymorphic crystallization process. However, if the energy states of the two polymorphs are very close to each other, the equilibrium-based methods may not be sufficient for the prediction of the preferred polymorph, and kinetic experiments have to be conducted in order to establish which polymorph will form under specific combination of temperature and solvent/antisolvent ratio.

In literature, several studies describe polymorph formation during an antisolvent crystallization process as a function of supersaturation changed by the solvent/antisolvent ratio. The effects of process parameters such as the initial solution concentration, temperature, or the injection rate of the antisolvent were investigated with regard to particle size distribution (PSD) of the final crystals. Park¹³ studied the antisolvent crystallization of carbamazepine from ethanol, while Kitamura¹⁴ investigated polymorphic antisolvent crystallization of thiazole-derivative (BPT) from methanol, with water as the antisolvent in both cases. The crystallization of polymorphs was found to depend most strongly on the water addition rate and the concentration of initial solution. Jiang¹⁵ studied the antisolvent crystallization of *o*-aminobenzoic acid by rapidly mixing ethanol solution with water. A low initial supersaturation provided the stable form I, while at high supersaturation the metastable form II was observed. Saleemi^{16,17} dealt with the modeling and monitoring of a combined cooling and antisolvent crystallization process. Their work illustrates the use of process analytical technology (PAT) tools, such as attenuated total reflectance ultraviolet visible (ATR-UV/vis)

spectroscopy and focused beam reflectance measurement (FBRM), for the monitoring of the crystallization mixtures of aminobenzoic acid isomers. Simone¹⁸ applied quantitative Raman spectroscopy and its calibration for the monitoring of *o*-aminobenzoic polymorphic transformation in the crystallization process. A recent review of the major developments in crystallization research, including the application of process monitoring tools, can be found in Nagy et al.¹⁹

The subject of the present work is the polymorphic crystallization of agomelatine (*N*-[2-(7-methoxy-1-naphthyl)-ethyl]acetamide), which is a novel antidepressant. Several (up to 11) polymorphic forms of agomelatine have been discovered to date. Agomelatine form II crystallizes as the most stable form at room temperature, while forms I and X can be prepared as metastable. Form I has been described by Tinant,²⁰ while several other polymorphs are mentioned in the patent literature, e.g., form II,²¹ form III,²² form IV,²³ form V,²⁴ form VI,²⁵ form X,²⁶ and form JR1–4.²⁷ In the Cambridge Structural Database, the crystal structures of three polymorphs of agomelatine can be found (forms I, II, and III).

In the present work, the influence of process conditions on the polymorphic antisolvent crystallization and transformations during cooling crystallization of agomelatine metastable form X from water/methanol solution has been investigated with a view of designing a robust process that includes not only crystallization but also filtration, filter cake washing, and drying. Agomelatine form X was selected on the basis of a patent situation. Success in the development of a robust preparation process of form X could bring the drug earlier to the market. Despite the fact that plenty of polymorphic forms have been discovered so far, the most stable form II and two metastable forms I and X can be predominantly observed during crystallization. While the crystallization from pure methanol provides the most stable form II, precipitation into pure water has been shown to lead to the formation of metastable forms (X and I). Thus, the methanol/water combination was chosen as a potentially suitable precipitation medium.

The competitive stability method was used in order to identify regions of the parametric space (water/methanol ratio, process temperature, and initial concentration) in which the crystallization of form X can be feasible. The formation of agomelatine form X was confirmed by subsequent kinetic experiments. The influence of process parameters such as the intensity of agitation, the antisolvent addition rate, and the precipitation temperature on the yield and particle size of the crystalline product was also investigated. The batch antisolvent crystallization of the metastable form X was monitored using in-line Raman spectroscopy and FBRM probe, and the type of the resulting polymorph has been confirmed by X-ray powder diffraction (XRPD). Finally, the effect of the obtained crystals of metastable form X on downstream operations—namely, filtration and drying—has been studied.

2. METHODOLOGY

2.1. Materials. The active pharmaceutical ingredients (agomelatine form I and X) were obtained from Sanofi (Turkey). Methanol (p.a.) was provided by Penta (Chrudim, Czech Republic). Agomelatine form II was obtained from solution by cooling crystallization as follows: 100 g (0.411 mol) of agomelatine form I was dissolved in 500 mL of methanol at 40 °C in an agitated 1 L glass vessel. The solution was cooled linearly down to 0 °C during 2 h and stirred for further 30 min at the final temperature. The resulting crystals were filtered,

washed, and dried overnight. The purchased and prepared solid forms were confirmed by X-ray analysis.

2.2. Solubility and Relative Stability. The relative stability without the presence of the solvent and the transition points between each polymorphic form were determined by DSC measurement according to eq 1 (Pyris 1, PerkinElmer). The sample of 3–4 mg agomelatine form I, II, or X was equilibrated at 50 °C and heated to 200 °C by a ramp of 10 °C/min. Nitrogen was used as a carrier gas with the flow rate of 20 mL/min.

The solubility and relative stability of agomelatine form I, II, and X in water/methanol solution at temperatures –30, –20, –10, 0, 10, and 20 °C was measured as a function of the methanol volume fraction in the range from 0 to 1. The water/methanol solution was saturated with the more soluble polymorphic form at a certain temperature. Afterward, the suspension was filtered and seeded by a mixture of each pair of polymorphic forms (I + II, I + X, or II + X). The suspension was stirred for 24 h in a 100 mL EasyMax reactor vessel (Mettler-Toledo, Germany). After 24 h, the suspension was filtered, and the concentration was determined gravimetrically. The solid phase was analyzed by XRPD.

2.3. X-ray Powder Diffraction Analysis. To resolve the structure of agomelatine form X, the powder sample was ground, placed into a 0.3 mm borosilicate glass capillary and measured in the transmission mode on the PANalytical Empyrean powder diffractometer from 4° to 80° 2θ with Cu $\text{K}\alpha_{1,2}$ radiation ($\lambda = 1.54184 \text{ \AA}$, focusing mirror, PIXCel^{3D} detector, step size was 0.013° 2θ, irradiated length of the capillary was 20 mm).

2.4. Combined Antisolvent/Cooling Crystallization Process. The formation kinetics of agomelatine form X was investigated in a combined antisolvent/cooling crystallization process, which consisted of two stages: a precipitation stage, followed by a cooling stage. During the precipitation stage, a solution of agomelatine in methanol (the solvent) from reactor 1 was added to water in reactor 2, which acted as the antisolvent. Additional crystal growth was then achieved by cooling of the suspension formed during the precipitation stage. The experimental setup of this process is shown in Figure 1.

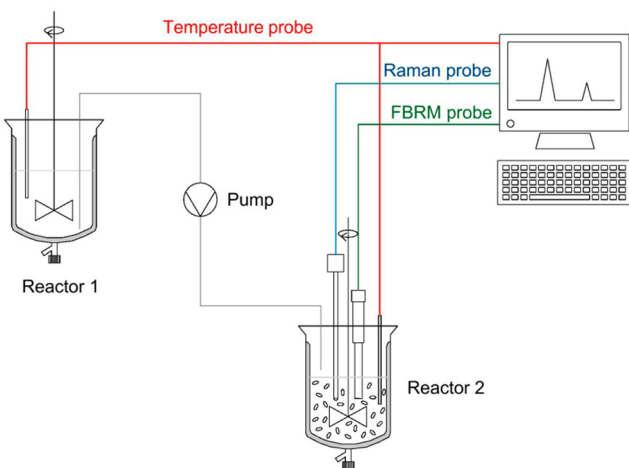


Figure 1. Schematic diagram of a 250 mL (Reactor 1) and 500 mL crystallizer (Reactor 2) with in-line Raman and FBRM probe.

Reactor 2 was equipped by an in-line FBRM probe (MetlerToledo) for chord length distribution and particle

concentration measurement and by a Raman probe (Kaiser Optical Systems, Inc.).

The reactor 2 was mixed by a three-blade impeller ($d/D = 0.5$, $h/H = 0.1$, diameter 0.064 m), which was set to 300 rpm. The stirrer speed was calculated from the power number N_p so as to achieve energy dissipation rate around 120 W/m^3 , which is recommended for antisolvent crystallization in this case, in order to obtain sufficient micromixing. In case of higher dissipation energy rate, the metastable zone width can be significantly reduced, leading to the crystallization of the undesirable more stable form (form II). The power number N_p is defined as²⁸

$$N_p = \frac{PV}{n^3 d^5 \rho} \quad (2)$$

where n is the rate of agitation (rpm), d is the diameter of agitator, ρ is the solution density, P is the energy dissipation rate per volume (W/m^3), and V is the volume of the liquid phase. For the type of impeller used, the value of N_p should be 0.4 in order to operate in a regime of fully developed turbulence. The temperature of reactors 1 and 2 was controlled by Huber CC 505 (Algochem) recirculators. The position of the feed tube in reactor 2 can also affect the antisolvent crystallization process. The feed tube was located just above the liquid level close to the impeller shaft in order to facilitate rapid dispersion of the added solution droplets and to avoid contact with the cooled reactor walls, which could lead to the formation of the stable form II.

The precipitation stage of the crystallization procedure consisted of adding the dissolved agomelatine in methanol (28 g in 100 mL) from reactor 1 into water or water/methanol mixture (250 mL) in reactor 2. The initial concentration of agomelatine in methanol in reactor 1 was constant in all cases and the solution was kept at 30 °C (saturated solution). The effect of the following parameters on the precipitation stage of the crystallization process was investigated: (i) composition of the antisolvent in reactor 2 (0 or 5 vol % of methanol in water), (ii) the addition rate of agomelatine solution from reactor 1 to reactor 2 (100 mL of the starting solution from reactor 1 was dropped into the antisolvent in reactor 2 during either 6 or 30 min, corresponding to addition rates of 4 and 20 mL/min, respectively), and (iii) the precipitation temperature in reactor 2, which was either +10 or 0 °C.

After the addition of the agomelatine methanol solution into reactor 2 was complete, the suspension in reactor 2 was exposed to different temperature profiles in order to influence the yield and final crystal size distribution; this was the cooling stage of the combined antisolvent/cooling crystallization process. When the precipitation was done at +10 °C, the final cooling temperature was either +10 °C (i.e., no cooling), 0 °C, or –10 °C. When the precipitation was done at 0 °C, the final cooling temperature was only –10 °C. Furthermore, in the case of cooling from +10 °C to –10 °C, two different cooling rates were investigated, namely, 20 and 40 °C/h.

Samples for XRPD analysis were taken during the crystallization process. At the end of the process, the crystals were filtered, and the filter cake was washed ($2 \times 200 \text{ mL}$) by cold distilled water and dried. The obtained material was analyzed by XRPD, optical microscopy, and scanning electron microscopy. The particle size distribution of the crystals was measured by static light scattering (Mastersizer 3000, Malvern Instruments, UK).

2.5. Agomelatine Form X Stability in Suspension with Final Composition of MeOH.

In a batch industrial process

after scale-up, the final crystalline product can reside in the solvent–antisolvent mixture for a significant amount of time before filtration. Therefore, the stability of agomelatine form X in the methanol–water (3:7) mixture was investigated at several temperatures in the range -10 to $+10$ °C. The composition of the mixture was chosen on the basis of the final methanol content (30%) in the suspension, formed after addition the entire agomelatine solution from reactor 1 to reactor 2 (i.e., after the precipitation stage). Part of the suspension was transferred to a smaller 100 mL EasyMax vessel and stirred for 24 h; samples were taken at the intervals 0.5, 1, 2, 4, 8, and 24 h and analyzed by XRPD.

2.6. Drying Procedure. Since filtration and drying are integral parts of the API crystallization and isolation process, and it is known that undesirable phase transitions can occur also during the drying step,²⁹ the influence of process parameters on the polymorphic transformation of agomelatine form X during drying was investigated as well. The methanol content in the filter cake before drying was analyzed by gas chromatography (GC). The amount of methanol was analyzed before and after washing the material by water (1× and 2× 200 mL of water per 25 g of wet cake). On the basis of obtained results, the samples containing 0, 1, 3, 10, 20, 30, and 40% of methanol were prepared and dried over 24 h at 30, 40, and 50 °C. The final polymorphic form was analyzed by XRPD.

3. RESULTS AND DISCUSSION

3.1. Polymorphs Identification. The polymorphic forms I, II, and X were analyzed by DSC (Figure 2), XRPD (Figure 3),

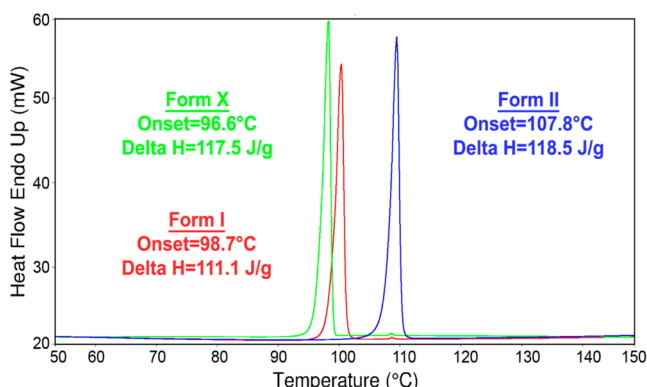


Figure 2. Melting points and enthalpies of fusion of agomelatine forms I, II, and X measured by DSC.

and Raman spectrometry (Figure 4). A full structure solution of agomelatine form X, which has not been described in the literature before, is given in Appendix I.

The success of polymorphic crystallization depends on differences in the solubility or in the melting points of each polymorphic form, which may occur during the crystallization process. Due to the similarity of melting points and heat of fusion values (Figure 2) belonging to forms I and X, it is likely that both forms will also have a similar solubility and probably a similar crystal structure as well. Although the XRPD patterns show distinct features for each of the three polymorphs (Figure 3), their Raman spectra (Figure 4) are almost identical. This means that the identification of the individual polymorphic forms during crystallization directly in the suspension by a Raman probe would not be sufficiently reliable, and therefore periodic

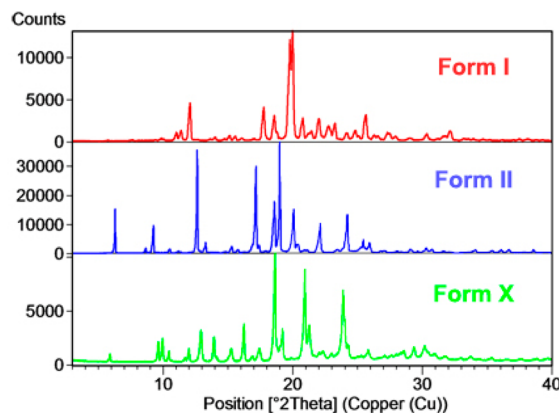


Figure 3. X-ray powder diffraction patterns of agomelatine form I, II, and X.

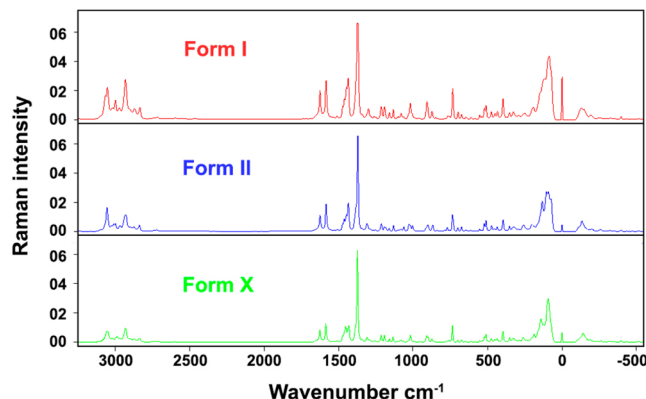


Figure 4. Raman spectra of agomelatine forms I, II, and X.

sampling of the suspension with off-line XRPD analysis was implemented as a way of monitoring polymorphic transitions during the crystallization process.

3.2. Solubility and Relative Stability. The melting points and heats of fusion of each polymorph are summarized in Table 1. On the basis of DSC measurement, agomelatine form

Table 1. Melting Points and Heat of Fusion Values for Agomelatine Polymorphic Forms I, II, and X

polymorphic form	I	II	X
melting point (°C)	98.7 ± 0.5	107.8 ± 0.5	96.6 ± 0.5
heat of fusion (J/g)	111.1	118.5	117.5

II should be the most stable polymorph at room temperature because of the highest melting point and heat of fusion value. Therefore, form II should be monotropically related to forms I and X. The melting points of forms I and X are very close to each other, and therefore eq 1 cannot be reliably applied. From experimental observation, it is known that form I is less stable and is transformed into more stable form X at room temperature. Since the relative stability among the polymorphs in the presence of a solvent is crucial for the successful design of a robust crystallization process, and depends on the solvent used, the relative stability was also evaluated by the competitive stability method. The relative stability of polymorphic forms in relation to the water/methanol ratio and temperature is summarized in Figure 5 for forms I + X and in Table 2, 3, and 4 for forms I + X, II + X, and I + II, respectively.

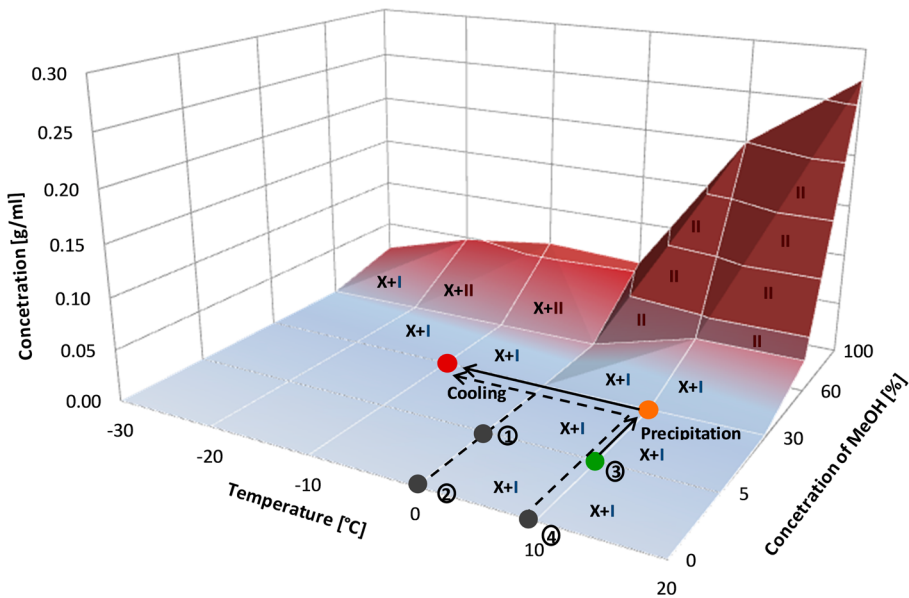


Figure 5. Relative stability of polymorphic forms in relation to methanol concentration in water and temperature. The region of the design space where form X does not transform into form II was selected for the crystallization process. The green point indicates the starting point of the precipitation stage; the red point indicates the end of the cooling phase. The gray points (1, 2, 3, and 4) and dashed arrows denote the individual crystallization process trajectories described in section 3.3.

Table 2. Relative Stability of Polymorphic Forms I + X in Relation to the Water/Methanol Ratio and Temperature

MeOH content (vol %)	temperature (°C)					
	-30	-20	-10	0	10	20
Concentration (g/mL)						
0				0.000	0.000	0.000
5		0.000	0.000	0.000	0.000	0.000
30		0.000	0.000	0.000	0.001	0.002
60	0.000	0.001	0.002	0.002	0.030	0.030
100	0.020	0.048	0.060	0.056	0.200	0.272
temperature (°C)						
MeOH content (vol %)	-30	-20	-10	0	10	20
Form						
0			I+X	I+X	I+X	
5	I+X	I+X	I+X	I+X	I+X	
30	I+X	I+X	I+X	I+X	I+X	
60	I+X	X+II	X+II	X+II	II	II
100	X+II	X+II	X+II	II	II	II

At higher concentration of methanol (60% and above), the polymorphic conversion of form X into the most stable form II has occurred. Therefore, this region of the parametric space was identified as not suitable for the crystallization process. On the other hand, in the region of methanol concentration up to 30%, the polymorphic transformation is significantly reduced at all investigated temperatures, which makes this region suitable for further kinetic studies. Due to low solubility and therefore limited diffusive transport, a 24 h period was not sufficient to conclusively establish whether form X or form I is more stable at any given temperature within this region, and the outcome of the crystallization process is likely to be kinetically rather than thermodynamically controlled. Therefore, several antisolvent/cooling crystallization scenarios were devised and investigated,

Table 3. Relative Stability of Polymorphic Forms II + X in Relation to the Water/Methanol Ratio and Temperature

MeOH content (vol %)	temperature (°C)					
	-30	-20	-10	0	10	20
Concentration (g/mL)						
0				0.000	0.000	0.000
5		0.000	0.000	0.000	0.000	0.000
30		0.000	0.000	0.000	0.001	0.001
60		0.000	0.000	0.000	0.002	0.032
100	0.001	0.046	0.067	0.112	0.200	0.270
temperature (°C)						
MeOH content (vol %)	-30	-20	-10	0	10	20
Form						
0				II+X	II+X	II
5			II+X	II+X	II+X	II
30			II+X	II+X	II	II
60	II+X	II+X	II+X	II	II	II
100	II+X	II+X	II+X	II	II	II

as indicated by the trajectories in Figure 5 and discussed in detail in the sections below.

3.3. Combined Antisolvent/Cooling Crystallization of Form X. The use of combined antisolvent/cooling crystallization process gains importance in cases where the application of cooling crystallization on its own is not possible, e.g., because of thermodynamic stability of the polymorph. The formation of a desired metastable form can be achieved by antisolvent crystallization (precipitation) at a temperature that allows the formation of the desired polymorph, and in case this temperature is not low enough to provide sufficient yield (loss of yield can be caused by higher solubility of the substance at the precipitation temperature), the suspension can be further cooled down in the second stage of crystallization that follows the initial antisolvent crystallization step. In that case, however,

Table 4. Relative Stability of Polymorphic Forms I + II in Relation to the Water/Methanol Ratio and Temperature

MeOH content (vol %)	temperature (°C)					
	-30	-20	-10	0	10	20
Concentration (g/mL)						
0				0.000	0.000	0.000
5		0.000	0.000	0.000	0.000	0.000
30		0.000	0.000	0.000	0.001	0.001
60	0.000	0.002	0.000	0.003	0.033	0.031
100	0.001	0.046	0.067	0.112	0.200	0.270
temperature (°C)						
MeOH content (vol %)	-30	-20	-10	0	10	20
Form						
0				II+I	II+I	II+I
5	II+I	II+I	II+I	II+I	II+I	II+I
30	II+I	II+I	II	II	II	II
60	II+I	II+I	II+I	II	II	II
100	II+I	II+I	II+I	II	II	II

the cooling crystallization stage bears a risk of crystallizing the more stable polymorph or the transformation of the desired (but metastable) polymorph formed during the antisolvent crystallization stage into a thermodynamically preferred polymorphic state at lower temperature. In the following sections, the individual crystallization procedures combining various conditions of both stages of crystallization (i.e., antisolvent and cooling) will be discussed.

3.3.1. Effect of Precipitation and Cooling Temperature.

The precipitation of agomelatine at 0 °C by dropping a methanol solution into the antisolvent (water with initial concentration of methanol either 0 and 5 vol %) is indicated in Figure 5 by the trajectories denoted by gray points 1 and 2. Figure 6a shows the evolution of methanol concentration and temperature over time and Figure 6b represents the particle count evolution for both cases. The dissolved agomelatine from reactor 1 was added dropwise into reactor 2 filled with pure water (green line) or water containing 5 vol % of methanol (blue line) during 30 min, which is the precipitation stage indicated in Figure 6a. The nucleation started immediately after addition of the first drops of agomelatine solution. The major variation of the total particle count within 30 min reflects the polymorphic transformation. Samples of crystals were taken each 10 min from the onset of the precipitation stage and analyzed by XRPD. The relative presence of individual polymorphic forms was evaluated from the relative intensity of their characteristic peaks (Figure 6c). It was observed that polymorph I is preferably formed at the beginning of precipitation, but during the later stages of the crystallization process, form I is converted into form V in the case of pure water being the antisolvent, or into form X when the antisolvent was a 5% methanol solution in water.

Precipitation at 0 °C caused the adhesion of material on the walls inside the reactor, presumably due to poor wettability of the precipitated particles by the solvent at this temperature. This adhesion is undesirable because the final yield (60%) is lower than that expected based on solubility difference.

In order to avoid adhesion of the freshly formed precipitate on the reactor walls and to increase the rate of conversion of form I, the precipitation temperature was increased to 10 °C

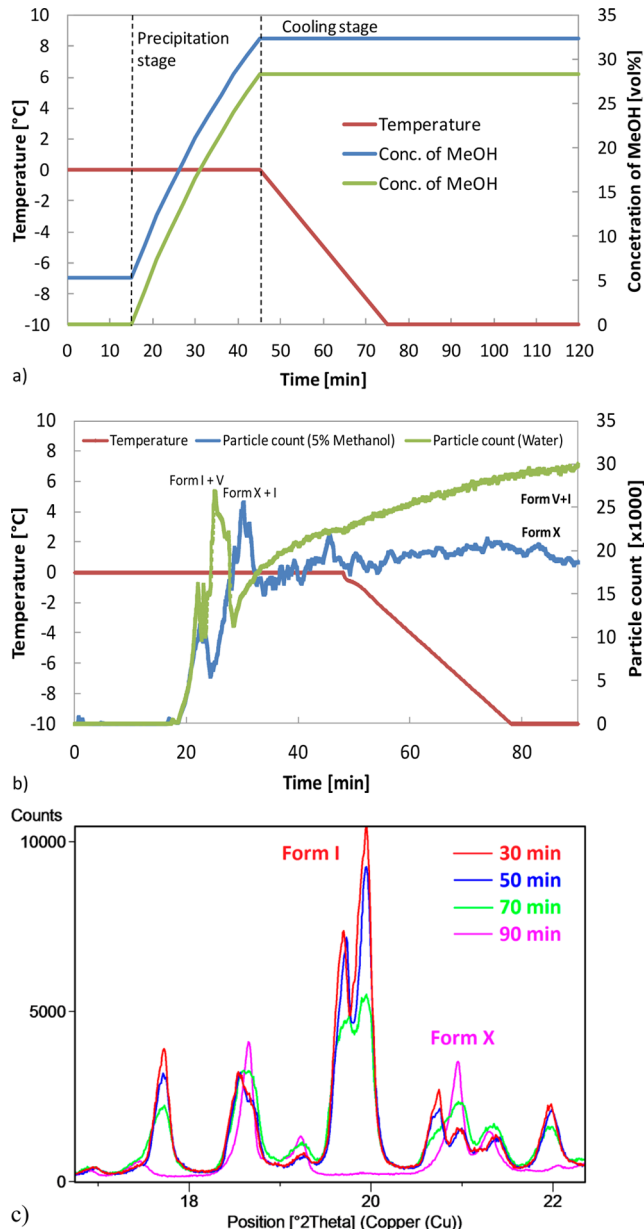


Figure 6. (a) Evolution of solvent composition (methanol concentration) and temperature over the time during the combined antisolvent/cooling crystallization process for precipitation at 0 °C followed by cooling to -10 °C. (b) Evolution of particle count measured by FBRM for the same process (the temperature curve is reproduced in order to relate the two graphs). (c) Transformation of metastable form I into more stable form X during the crystallization process with 5% methanol as the antisolvent.

(trajectories indicated by points 3 and 4 in Figure 5) with all other parameters being constant (i.e., two compositions of antisolvent, same dropping time of 30 min, same final cooling temperature of -10 °C). Under these conditions (Figure 7b), XRPD measurements revealed that a mixture of forms I and X was formed in case of precipitation into pure water (green line) at the beginning of precipitation. The rapid decrease of total particle count that follows after the initial nucleation stage where a mixture of forms I and X was formed is probably a consequence of dissolution of form I and its transformation into form X, which continues to nucleate. In the case of precipitation into 5 vol % of methanol solution, the formation

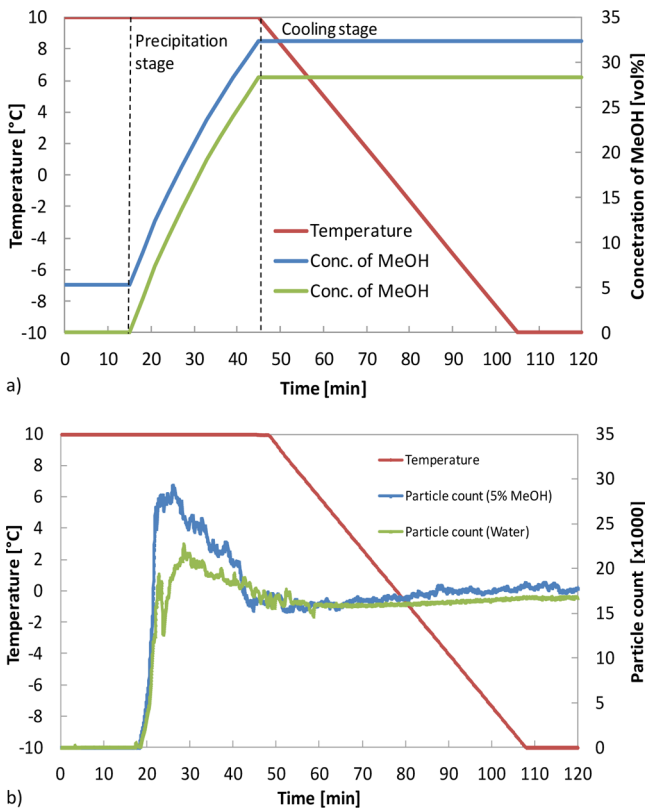


Figure 7. (a) Evolution of methanol concentration and temperature over the time for precipitation at 10 °C followed by cooling to -10 °C. (b) Evolution of particle count (measured by FBRM) for the same process.

of form X was observed since the onset of nucleation, and no intermediate decrease of particle count was observed. As the methanol concentration increases during later stages of precipitation, the overall particle count decreases in the case for both antisolvent compositions most likely due to redissolution of some of the nuclei and ripening of the crystals (agglomeration of crystals, which could also explain the decrease of particle count, was not observed). XRPD analysis revealed that the final product contained only form X. The higher temperature (10 °C instead of 0 °C) reduced the adhesion of material on the walls of the reactor, and due to this, the final yield was 98% (note that the final cooling temperature was the same as in the previous case, i.e., -10 °C). Furthermore, the material was nonagglomerated with a high physical quality.

From the experiments described above, it follows that a nearly 100% yield can be obtained when the precipitation temperature was 10 °C and the final cooling temperature was -10 °C. However, for practical and economical reasons, it may be desirable to carry out the cooling stage of the combined crystallization process at a higher temperature, or possibly to even avoid the cooling stage entirely. Therefore, the influence of the final temperature on the yield of crystallization was investigated. All parameters remained constant (i.e., the precipitation temperature was 10 °C, and the antisolvent was a 5 vol % methanol solution in water) except the final temperature of the cooling step, which was increased to either 0 °C or +10 °C (i.e., no cooling at all after precipitation). In both cases, the yield decreased only slightly and was 96%, which means that for these conditions the yield is predominantly controlled already by the first (antisolvent crystallization)

stage of the process. However, the polymorphic form and the yield are not the only performance criteria of the process. Also the crystal size distribution is of interest, which can be controlled by the rate of precipitation and the rate of cooling.⁴

3.3.2. Effect of Precipitation and Cooling Rate. The influence of cooling rates (20 and 40 °C/h) from the precipitation temperature of +10 °C to the final cooling temperature of -10 °C on particle size distribution was investigated. The progress of temperature, methanol concentration, and particle count during this experiment is summarized in Figure 8, and the resulting particle size distribution is shown in Figure 9.

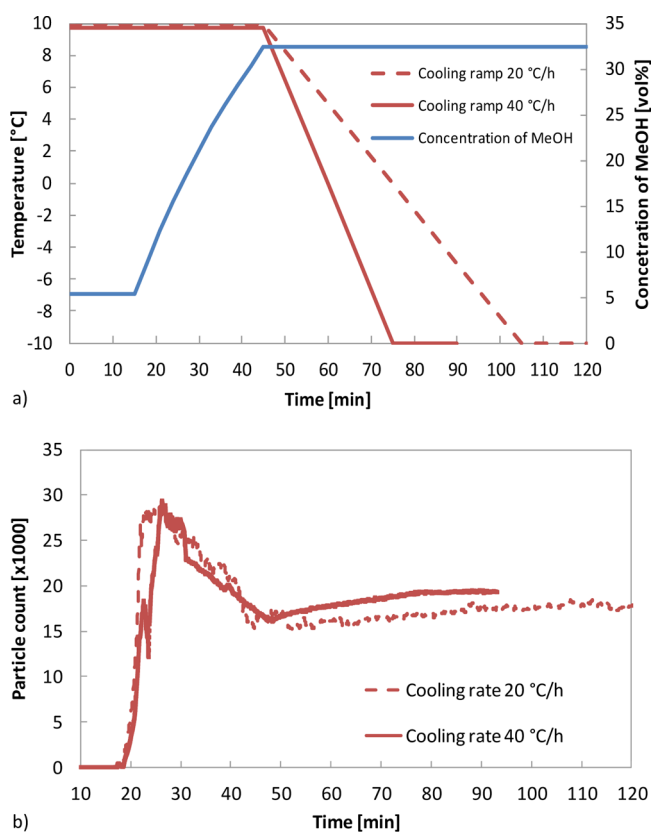


Figure 8. (a) Evolution of temperature and methanol concentration over the time for two cooling rates 20 °C/h (dashed line) and 40 °C/h (solid line).

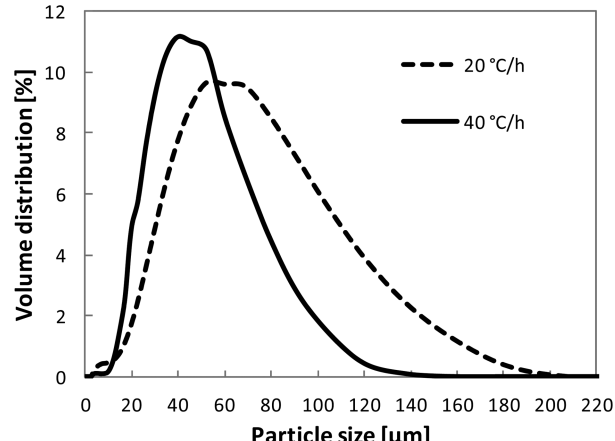


Figure 9. Particle size distribution of different cooling rates 20 and 40 °C/h.

In the case of cooling rate 20 °C/h, the particle count was slightly lower, and the particle size was shifted toward larger values in comparison with the cooling rate 40 °C/h at the end of the crystallization process. The decrease of particle count and larger PSD can be explained by ripening of the crystals that were initially formed during the precipitation stage. The slower cooling rate of 20 °C/h (dashed line in Figure 8a) provided an opportunity for the crystals to grow for a longer period of time. On the other hand, the cooling rate of 40 °C/h did not provide sufficient time for the ripening process to take place, and the resulting particles had a smaller PSD.

While crystal ripening during the cooling stage can influence the PSD of the final crystals, the starting PSD is determined by the conditions of the precipitation stage. Hence, the influence of the addition rate of the methanol solution in the antisolvent was investigated by changing the addition rate from the base value of 4–0 mL/min. In the case of the addition rate 4 mL/min the addition time of the entire agomelatine solution into the antisolvent was 30 min, and in case of the rate 20 mL/min the addition was carried out during 6 min (Figure 10a). After

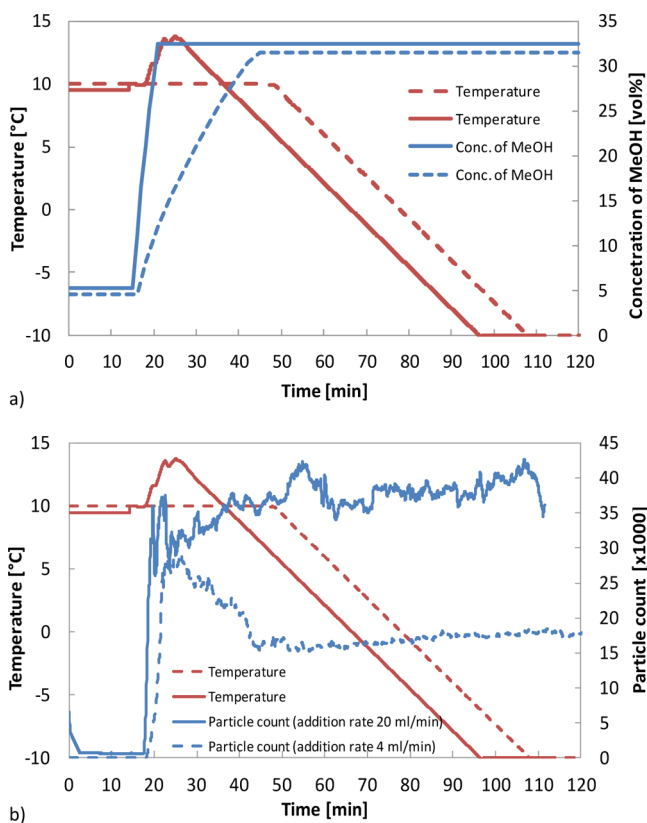


Figure 10. (a) Evolution of temperature and methanol concentration over the time for two addition rates of agomelatine solution into the antisolvent, 20 mL/min (solid line) and 4 mL/min (dashed line). (b) Evolution of particle count during the process for the two addition rates, measured by FBRM.

addition of dissolved agomelatine in methanol, the cooling was commenced at the default rate of 20 °C/h, and the final temperature was −10 °C. Note that for the fast addition rate (20 mL/min) the recirculator was no longer able to maintain constant temperature of the receiving solution and the temperature temporarily rose above the set value of 10 °C (recall that the agomelatine solution had 30 °C). The particle count during the process was again monitored by FBRM

(Figure 10b), and the PSD of the final crystals was evaluated by static light scattering (Figure 11).

The crystals formed during the addition rate of 20 mL/min were significantly smaller than those formed at 4 mL/min, which is revealed not only by their PSD (Figure 11) but also by

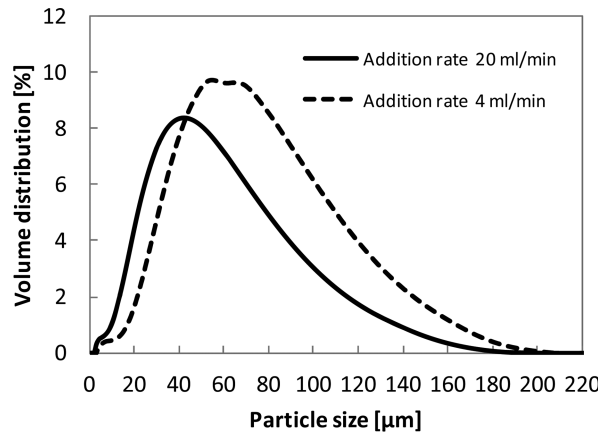


Figure 11. Particle size distribution of final crystals obtained for different addition rates, 20 and 4 mL/min.

SEM analysis (Figure 12). Since the overall yield on a mass basis was identical in both cases (98%), a smaller particle size should imply a larger number of particles, which is indeed the case. The particle count measured by FBRM during the process was nearly twice higher in the case of the fast addition rate (Figure 10b). Interestingly, the particle count did not decrease during the subsequent cooling stage, which would imply that crystal ripening during the cooling stage occurs only to a limited extent and the main parameter that controls the PSD is the addition rate into the antisolvent during the precipitation stage.

3.4. Agomelatine Form X Stability in Suspension and Drying. Since crystallization is typically followed by a filtration step during the manufacturing process, and the crystals can remain in the slurry for some time before the filtration begins, it is of interest to investigate the stability of agomelatine form X in the slurry. Obviously, any uncontrolled polymorphic transitions would be undesirable at this stage. Therefore, agomelatine form X was stirred in the methanol/water mixture (3:7 by volume, which corresponds to the solvent composition at the end of the antisolvent crystallization step) at the temperatures −10, −5, 0, 5, and 10 °C for 24 h. Samples of the solid form were analyzed by XRPD at time intervals 0.5, 1, 2, 4, 8, 24 h. In all cases, the polymorph of agomelatine form X was confirmed, for all temperatures. The solubility of agomelatine form X in a 30% methanol solution is practically negligible, and therefore mass transfer via the solution does not favor recrystallization into other, more stable forms, within 24 h. The stability of agomelatine form X in a 30% methanol solution for 24 h is a relevant advantage from the scale-up and manufacturing point of view, where the procedural steps are temporally demanding.

To investigate the effect of drying on possible polymorphic transitions, the crystals of agomelatine form X were first filtered through a frit and exposed to washing steps by water. The wet filter cake before washing contained 3.00% of methanol, which implies a moisture content of 10% since the filtrate was a 3:7 methanol–water solution. When the filter cake was washed by

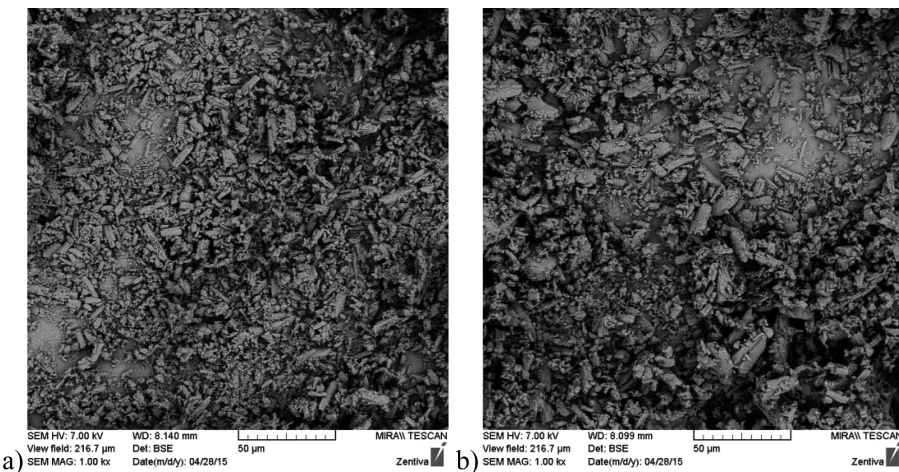


Figure 12. SEM micrographs of final crystals obtained for addition rate of (a) 20 mL/min and (b) 4 mL/min.

cold water (1×200 mL/25 g), the methanol content was reduced to 1.30%, and when the washing step was applied twice (2×200 mL/25 g), the methanol content decreased further to 0.05%. Assuming that the moisture content of the wet cake on the frit was the same after each washing step, the composition of the solvent was changed to 0.05:9.95 methanol–water ratio. The washed material was then dried in air at laboratory temperature. The residual methanol content in the dried material was 0.00%, and its polymorphic form was confirmed by XRPD to be form X.

In order to simulate conditions of imperfect washing, the dried samples of agomelatine form X were mixed with pure methanol so as to contain 0, 1, 3, 10, 20, 30, and 40% of methanol on mass basis. Each of these samples was then vacuum-dried at 30, 40, and 50 °C and analyzed by XRPD. For all three temperatures, all samples except those with 0% of added methanol transformed into pure stable form II. These results are perhaps not too surprising in the cases where a higher methanol content was used, because the polymorphic transformation could occur via the dissolution-recrystallization route (cf. Figure 5). However, for 1% of added methanol, the powder was still essentially a free-flowing “dry” powder, and the complete conversion to form II still occurred. Presumably, the polymorphic transformation took place in the solid state and was only facilitated by the presence of methanol vapors. This means that good washing by water prior to drying is a crucial step if the metastable agomelatine form X produced by antisolvent crystallization is to be preserved during drying. On the basis of these results, the washing of filter cake by cold water (at least 2×40 mL/1 g) and predrying at room temperature is recommended before the final vacuum drying at higher temperatures.

CONCLUSIONS

A metastable polymorphic form (form X) of agomelatine has been identified; its structure has been fully characterized, and a robust process for producing this form has been developed. The process combines antisolvent and cooling crystallization steps, and the influence of several process parameters, namely, the antisolvent composition, the antisolvent temperature, the antisolvent addition rate, the cooling rate, and the final cooling temperature on the purity and yield of the polymorphic form X, has been systematically investigated. The crystallization process was monitored online by a FBRM probe, which was

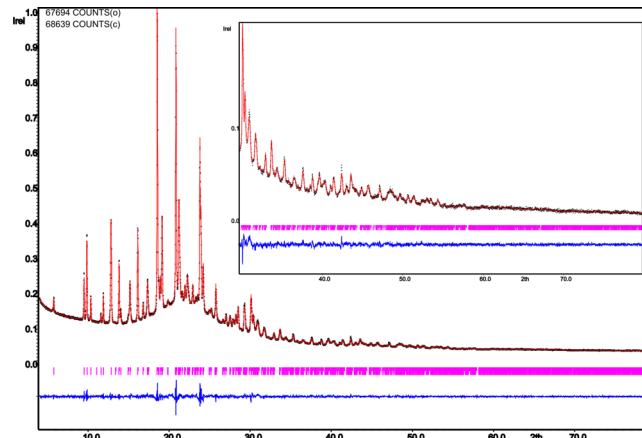


Figure 13. Final Rietveld plot showing the measured data (black thin-cross), calculated data (red line), and difference curve (blue line). Calculated Bragg positions are shown by vertical bars.

Table 5. Crystallographic Data and Details of Structure Refinement

chemical formula	C ₃₀ H ₃₄ N ₂ O ₄
formula weight	486.6
crystal system, space group	monoclinic, P2 ₁ /n
Z	4
a, Å	30.8643(7)
b, Å	9.3763(3)
c, Å	9.40306(19)
β, deg	98.5807(7)
V, Å ³	2690.71(11)
R _p	0.0167
R _{wp}	0.0218
R _{exp}	0.0133
S	1.64
Λ	1.5418 Å (Cu Kα)
2θ _{min} , 2θ _{max} , deg	4.00, 79.99
increment in 2θ, deg	0.013
nb. restraints	88
nb. constraints	171
refined parameters	148
Δρ _{min} , Δρ _{max} , eÅ ⁻³	-0.14, 0.10

Table 6. Comparison of Unit Cell Parameters and Length of Hydrogen Bonds in Forms I, II, and X

	<i>a</i> (Å)	<i>b</i> (Å)	<i>c</i> (Å)	β (deg)	<i>V</i> (Å ³)	N···O (Å)
Form I	31.501(4)	9.528(1)	17.906(2)		5374.3(11)	2.852 (8), 2.891 (7), 2.896 (8)–2.927 (8)
Form II	15.4300(12)	9.2934(7)	20.8558(13)	115.241(4)	2705.1(3)	2.843 (3), 2.860 (3)
Form X	30.8643(7)	9.3763(3)	9.40306(19)	98.5807(7)	2690.71(11)	2.784 (9), 2.904 (9)

complemented by off-line analysis of particle size distribution (laser scattering) and crystal structure (XRPD). The obtained polymorphic form was dependent mainly on the conditions of the antisolvent crystallization step, whereas the final yield and particle size of the crystalline product were influenced also by the conditions of the cooling step. In pharmaceutical technology, crystallization is typically followed by filtration, washing and drying. The influence of these steps on the final product properties was therefore investigated as well. While the suspension of crystals of form X in the mother liquor (30% of methanol in water) was stable for 24 h over a range of temperatures and drying from a filter cake washed by pure water did not lead to any polymorphic transitions, the crystals were found to be highly sensitive to the presence of pure methanol even in small amounts, which lead to a rapid conversion to the thermodynamically more stable agomelatine form II. Thus, this work has shown that a metastable form X can be produced and isolated by a well-chosen trajectory through the composition–temperature space, and it has also identified the parametric sensitivity of the process, in line with the Quality by Design philosophy.

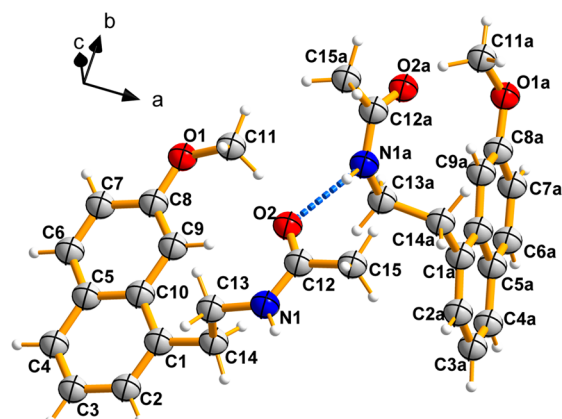


Figure 14. An ORTEP view of form X showing the asymmetric unit cell with the indication of the hydrogen bonding, atomic numbering and displacement spheres, which are drawn at 50% probability level.

APPENDIX I: STRUCTURE SOLUTION OF AGOMELATINE FORM X

The crystal structure of agomelatine form X was solved from powder X-ray diffraction data. Since agomelatine form X is a metastable polymorph obtained only kinetically by antisolvent precipitation, it was not possible to obtain a suitable single crystal. Therefore, the structure solution from powder data was utilized. The indexation in Conograph³⁰ and subsequent Le Bail fitting in JANA2006³¹ software found the monoclinic unit cell $a = 30.8643(7)$ Å, $b = 9.3763(3)$ Å, $c = 9.40306(19)$ Å and $\beta = 98.5807(7)^\circ$, $V = 2690.71(11)$ Å³ with space group $P2_1/n$. By comparing the volume of the unit cell with the approximate volume of agomelatine, it is clear that the asymmetric part of the unit cell contains two molecules of agomelatine. The crystal structure was solved by using parallel tempering algorithm as it is implemented in program FOX³² with two independent molecules in the asymmetric part of the unit cell. The molecular model of agomelatine was separated from the already known crystal structure with CSD ref code WERNOW01.

The suggested crystal structure by FOX was refined in JANA2006 software. The final refinement allowed refining positions and one isotropic ADP parameter of all non-hydrogen atoms (hydrogen atoms were kept in their theoretical positions) together with profile parameters, zero-shift, background, and unit cell parameters. The molecular model had to be restrained with soft bonds and bond-angles restraints (tolerance was set to 0.001 for bonds and 0.01 for angles) to get the result with reasonable molecular geometry. Values of restraints were calculated from the known crystal structure with CSD ref code WERNOW01.³³ The final agreement profile factors are $R_p = 1.67\%$, $R_{wp} = 2.18\%$, and $GOF = 1.64$. Details of measurement and refinement are given in Table 5, and the final plot is shown in Figure 13.

Even if using bond and bond angle restraints during refinement of the form X disallow us studying real values of bond and angles it still allows us to study and compare the final molecular shape and molecular packing, respectively. All already known polymorphic forms of Agomelatine I, II, and X differ in

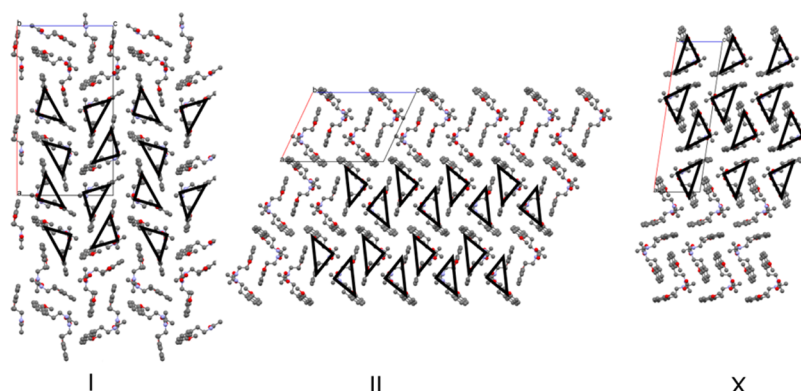


Figure 15. Comparison of crystal packing of agomelatine forms I, II, and X in the *a*–*c* plane; the triangles represent the infinite chains of H-bonded molecules going along *b*-axis.

unit cell parameters and space groups, but the molecular packing in all of these forms is based on the same hydrogen bonding system, where molecules of agomelatine are connected to the infinite chains by a single N–H···O interaction; see Table 6. All forms of agomelatine differ only in the packing of these infinite chains, which are connected together by different interactions, namely, π – π and π –H, see Figure 14 and 15.

To compare the densities, the data for all three polymorphs at the room temperature have been taken, since it was the temperature, at which all of the structures were determined. When the densities were compared with each other (Table 7), it was found, however, that they are basically the same.

Table 7. Density of Agomelatine Forms I, II, and X Calculated from Their Crystal Structures at Room Temperature

polymorphic form	I	II	X
density (g/cm ³)	1.2028	1.1948	1.2021

Therefore, it is not possible to determine the relative stability of the agomelatine polymorphs based on their density. The density rule applies in most cases, but certainly not in all.

AUTHOR INFORMATION

Corresponding Author

*E-mail: frantisek.stepanek@vscht.cz; phone: +420 220 443 236.

Notes

The authors declare no competing financial interest.

ACKNOWLEDGMENTS

Financial support from the Specific University Research (MSMT 20/2015) is gratefully acknowledged. F.S. would like to acknowledge support from the Grant Agency of the Czech Republic (project no. 15-05534S).

NOTATION

<i>d</i>	Diameter of agitator, m
ΔH_f	Heat of fusion, J/g
<i>T</i> _{mp}	Melting point temperature, °C
<i>N</i> _p	Power number
<i>P</i>	Energy dissipation rate per volume, W/m ³
<i>n</i>	Rate of agitation, rpm
<i>T</i> _t	Transition point, °C
<i>V</i>	Volume of the liquid phase, m ³
ρ	Density of stirred material, kg/m ³

REFERENCES

- (1) Sypek, K.; Burns, I. S.; Florence, A. J.; Sefcik, J. *J. Cryst. Growth Des.* **2012**, *12*, 4821–4828.
- (2) Roelandts, C. P. M.; Jiang, S.; Kitamura, M.; ter Horst, J. H.; Kramer, H. J. M.; Jansens, P. J. *J. Cryst. Growth Des.* **2006**, *6*, 955–963.
- (3) Qu, H.; Alatalo, H.; Hatakka, H.; Kohonen, J.; Louhi-Kultanen, M.; Reinikainen, S.-P.; Kallas, J. *J. Cryst. Growth* **2009**, *311*, 3466–3475.
- (4) Holáň, J.; Ridvan, L.; Billot, P.; Štěpánek, F. *Chem. Eng. Sci.* **2015**, *128*, 36–43.
- (5) Mullin, J. W. Solutions and solubility. *Crystallization*, 4th ed.; Butterworth-Heinemann: Oxford, 2001; pp 86–134.
- (6) Tung, H.-H.; Paul, E. L.; Midler, M.; McCauley, J. A. Polymorphism. *Crystallization of Organic Compounds*; John Wiley & Sons, 2008; pp 49–76.
- (7) Tung, H.-H.; Paul, E. L.; Midler, M.; McCauley, J. A. Special Applications. *Crystallization of Organic Compounds*; John Wiley & Sons, 2008; pp 235–277.
- (8) Kitagorodskii, A. I. *Organic chemical crystallography*; Consultants Bureau: New York, 1961.
- (9) Bernstein, J. *Polymorphism in molecular crystals*; Oxford University Press, 2007.
- (10) Nelyubina, Y. V.; Glukhov, I. V.; Antipin, M. Y.; Lyssenko, K. A. *Chem. Commun.* **2010**, *46*, 3469–3471.
- (11) Burger, A.; Ramberger, R. *Microchim. Acta* **1979**, *72*, 273–316.
- (12) Katrincic, L. M.; Sun, Y. T.; Carlton, R. A.; Diederich, A. M.; Mueller, R. L.; Vogt, F. G. *Int. J. Pharm.* **2009**, *366*, 1–13.
- (13) Park, M.-W.; Yeo, S.-D. *Chem. Eng. Res. Des.* **2012**, *90*, 2202–2208.
- (14) Kitamura, M. *J. Cryst. Growth* **2002**, *237*–239, 2205–2214.
- (15) Jiang, S.; ter Horst, J. H.; Jansens, P. *J. Cryst. Growth Des.* **2008**, *8*, 37–43.
- (16) Saleemi, A. N.; Rielly, C. D.; Nagy, Z. K. *Chem. Eng. Sci.* **2012**, *77*, 122–129.
- (17) Nagy, Z. K.; Fujiwara, M.; Braatz, R. D. *J. Process Control* **2008**, *18*, 856–864.
- (18) Simone, E.; Saleemi, A. N.; Nagy, Z. K. *Chem. Eng. Res. Des.* **2014**, *92*, 594–611.
- (19) Nagy, Z. K.; Fevotte, G.; Kramer, H.; Simon, L. L. *Chem. Eng. Res. Des.* **2013**, *91*, 1903–1922.
- (20) Tinant, B.; Declercq, J.-P.; Poupaert, J. H.; Yous, S. *Acta Crystallogr., Sect. C: Cryst. Struct. Commun.* **1994**, *50*, 907–910.
- (21) Souvie, J. C.; Gonzalez-Blanco, I.; Thominot, G.; Chapuis, G.; Horvath, S.; Damien, G. Process for the synthesis and crystalline form agomelatine. US7544839, Servier Lab [FR], 2009.
- (22) Coquerel, G.; Linol, J.; Souvie, J. C. Crystalline form III of agomelatine, a process for its preparation and pharmaceutical compositions containing it. US7635721, Servier Lab [FR], 2009.
- (23) Coquerel, G.; Linol, J.; Souvie, J. C. Crystalline form IV of agomelatine, a process for its preparation and pharmaceutical compositions containing it. US2006270875, Servier Lab [FR], 2010.
- (24) Coquerel, G.; Linol, J.; Souvie, J. C. Crystalline form V of agomelatine, a process for its preparation and pharmaceutical compositions containing it. US2006270877, Servier Lab [FR], 2006.
- (25) Coquerel, G.; Linol, J.; Pape, L. L.; Lecouve, J. P. Cystalline form VI of agomelatine, a process for its preparation and pharmaceutical compositions containing it. US2009069434, Servier Lab [FR], 2009.
- (26) Tombari, D. G.; Mangone, C. P.; Garcia, M. B.; Vecchioli, A.; Labriola, R. A.; Burton, G.; Rustoy, E. M. New process for the preparation of n-[2-(7-methoxy-1-naphthyl)-ethyl]acetamide and new crystalline form. WO2011154140, Gador SA [AR], 2011.
- (27) Dammer, O.; Rezac, J.; Richter, J.; Ridvan, L. Metastable crystal forms of agomelatine. WO2012097764, Zentiva k.s [CR], 2012.
- (28) Couper, J. R.; Penney, W. R.; Fair, J. R.; Walas, S. M. Mixing and Agitation. *Chemical Process Equipment*, 2nd ed.; Gulf Professional Publishing: Boston, 2010; pp 273–324.
- (29) Tung, H.-H.; Paul, E. L.; Midler, M.; McCauley, J. A. Properties. *Crystallization of Organic Compounds*; John Wiley & Sons, 2008; pp 13–47.
- (30) Oishi-Tomiya, R. *J. Appl. Crystallogr.* **2014**, *47*, 593–598.
- (31) Petříček, V.; Dušek, M.; Palatinus, L. *Z. Kristallogr. - Cryst. Mater.* **2014**, *229*, 345.
- (32) Favre-Nicolin, V.; Černý, R. *J. Appl. Crystallogr.* **2002**, *35*, 734–743.
- (33) Zheng, S.-L.; Chen, J.-M.; Zhang, W.-X.; Lu, T.-B. *Cryst. Growth Des.* **2011**, *11*, 466–471.